Polymer Bulletin 59, 855–864 (2008)
DOI 10.1007/s00289-007-0831-4

Polymer Bulletin

Mechanical Property, Thermal Property and Crystal Structure of Isotactic Polypropylene Samples Prepared by Vibration Injection Molding

Jie Zhang (✉), Ji Zhu, Yanwei Lei, Tai Zeng, Kaizhi Shen (✉), Qiang Fu

College of Polymer Science & Engineering, State Key Laboratory of Polymer Materials Engineering, Sichuan University, Chengdu, 610065
E-mail: zhaolanr@163.com

Received: 5 June 2007 / Revised version: 6 August 2007 / Accepted: 22 August 2007
Published online: 13 September 2007 –

Abstract

A self-designed pressure vibration injection device was used to study the effect of vibration frequency and vibration pressure on tensile strength and impact strength of iPP F401 vibration injection molding samples. Furthermore, vicat softening temperature, WAXD measurements and polarized microscopic observation were conducted. According to the results, tensile strength and impact strength increase with increasing vibration frequency and vibration pressure. The maximum increment of tensile strength is 26.1%. Under certain process conditions, there is a transition of the impact strength, whose maximum increment is 85%. The vicat softening temperatures have a significant increase of 6~8°C for the samples obtained at high vibration frequencies compared with that of static samples. According to pole figures, α-PP of vibration samples orientates much stronger than that of static samples. PM micrograghs show that vibration changes the crystal structure of samples and enhances their orientation.

Keywords

vibration injection molding; iPP; thermal property; mechanical property; crystal structure

Injection molding is one of the main polymer processing methods. The structure of parts prepared by conventional injection molding is of skin-core structure, it is hard to control the morphology and mechanical property of the parts. However, when additional energy field is added in the process of injection molding, the mechanical property of injection parts can be enhanced via increasing orientation of polymer molecular chains of the core under appropriate processing conditions [1-2]. Vibration field, which is a kind of special energy field, can be used in the process of injection molding to change the rheological behavior of polymer melt and polymer morphology when proper vibration parameters, such as vibration frequency and vibration intensity, and processing conditions are used, and the performance of polymer parts are improved [3-6]. To study the effect of vibration conditions on mechanical property

and crystal structure of Isotactic Polypropylene (IPP), we carried on experiments of vibration-injection molding using a self-designed pressure vibration equipment with vibration frequency of 0~1.5Hz and vibration pressure of 0~75MPa.

1. Experimental

Material

IPP F401 used in the experiment was commercialized products from Lan Gang petroleum chemical, China, $Mw = 7.8x10^4$, MFI = 1.87g/10min.

Samples preparation and characteration

The schematic representation of the pressure vibration equipment is shown in Figure 1. In our experimental of vibration injection molding, IPP was melted and extruded into the barrel first, and then injected into the mold cavity under the action of the piston that would vibrate during the stages of injection and packing. When the piston vibrated, an additional pulsation pressure, which changed from zero to its maximum periodically, was introduced to polymer melt in the cavity. We use the term vibration pressure to represent its maximum value. Three parameters, including melt temperature (T), vibration frequency (f) and vibration pressure (Pv), were changed in our experiment. The processing parameters were: injection pressure and packing pressure were 40MPa, melt temperature was 190°C /210°C /230°C, mold temperature was 60°C, vibration pressure was from 0 to 75MPa, and vibration frequency was from 0 to 1.5Hz.

A Shimadzu universal testing machine, Model AG-10TA, was used for tensile testing at room temperature (23°C). The crosshead speed was 50mm/min. A Charpy-type impact machine was employed to do impact testing at room temperature (23°C). The impact speed was 2.9m/s. A Model RW-3 Vicat heat resistance instrument was used to test the Vicat softening temperatures of samples. Silicone-oil was used as heating medium. The speed of temperature increase was 12°C/min. A Brvker D8 diffractometer with a texture attachment was used to obtain the data for 3D pole figures. A polarization microscope, model LEICA DMLP, was used to observe the microstructure of samples.

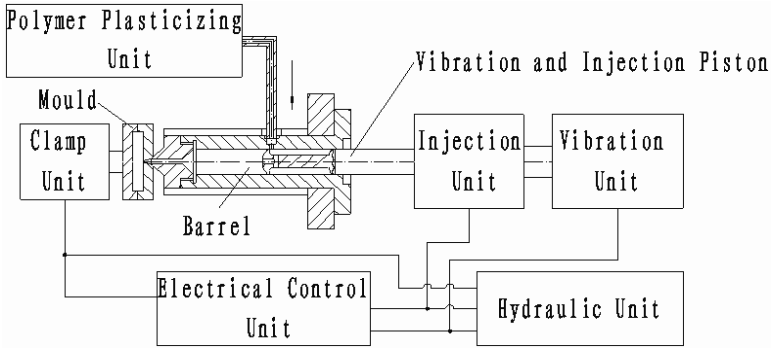

Figure 1. The schematic representation of vibration injection molding.

2. Results

Mechanical properties

The effect of vibration frequency on tensile strength and impact strength of vibration samples are showed in Figure 2 and Figure 3. The samples were obtained at Pv = 15MPa with different melt temperatures. Tensile strength of samples increases with increasing vibration frequency, but samples obtained at the different melt temperature have different increment. The maximum increments of tensile strength are 20.8%, 16.0% and

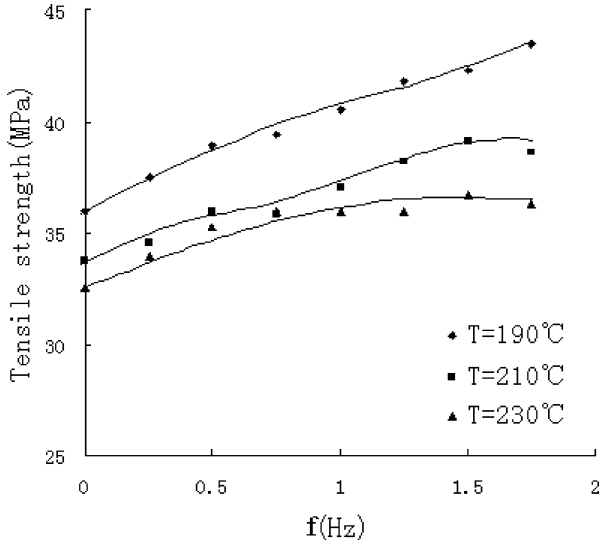

Figure 2. The effect of vibration frequency on tensile strength.

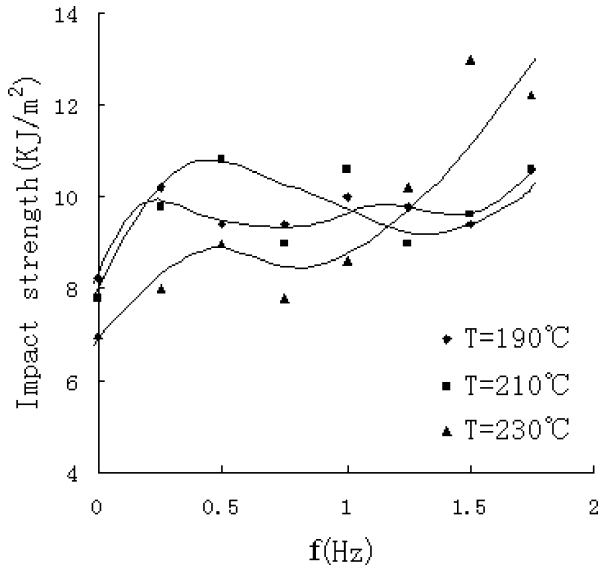

Figure 3. The effect of vibration frequency on impact strength.

14.5% respectively. Impact strength of the samples also increases with increasing vibration frequency. It should be noted that the impact strength of samples, which were obtained at T = 230°C, increase significantly at high vibration frequencies.

The effect of vibration pressure on tensile strength and impact strength of vibration samples are showed in Figure 4 and Figure 5. The samples were obtained at f = 0.5Hz with different melt temperatures. Tensile strength of vibration samples increases with increasing vibration pressure, but samples obtained at the different melt temperatures have different increments. The maximum increments of tensile strength are 26.1%, 22.0% and 18.5% respectively. When vibration pressure is low, impact strength of

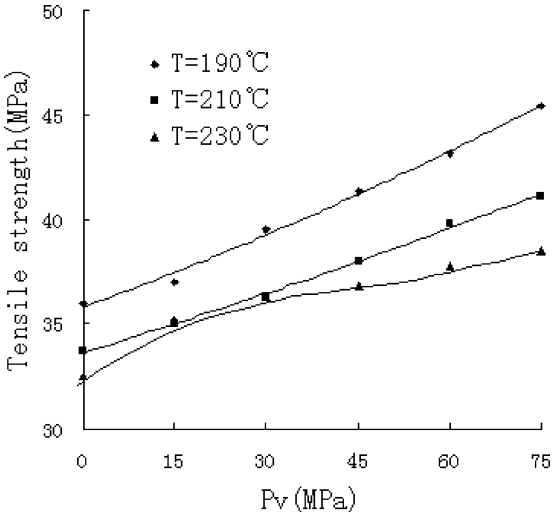

Figure 4. The effect of vibration pressure on tensile strength.

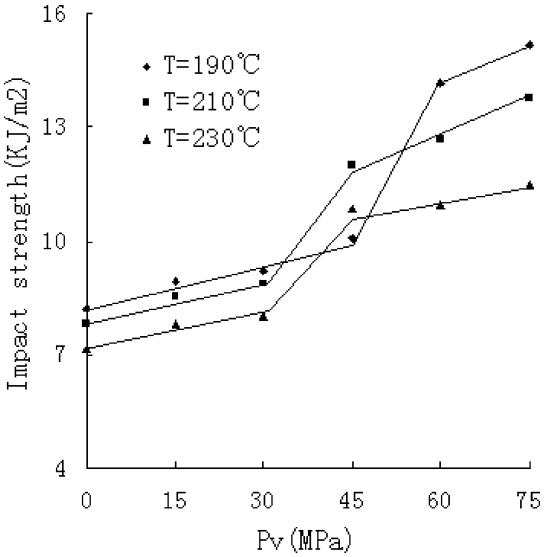

Figure 5. The effect of vibration pressure on impact strength.

samples increases slowly with increasing vibration pressure. At higher vibration pressure, there is a transition for impact strength as vibration pressure increases. However, as vibration pressure continues to increase, the increase of impact strength slows down. The maximum increments of impact strength are respectively 85%, 77% and 60% for the samples obtained at different molding temperatures of 190°C, 210°C and 230°C.

Vicat softening temperature

Table 1 shows the test results of vicat softening temperatures of samples obtained under different process conditions. According to the results, vicat softening temperature has a significant increase of 6~8°C for the samples obtained at high vibration frequencies compared with that of no-vibration samples, and for the samples obtained at low vibration frequencies, vicat softening temperature almost has no increase even if the vibration pressure is very high.

Table 1 vicat softening temperature of selected samples

melt temperature (°C)	vibration frequency (Hz)	vibration pressure (MPa)	vicat softening temperature (°C)
190	no vibration		98
190	1.5	35	104
190	0.5	75	100
230	no vibration		99
230	1.5	35	107
230	0.5	75	97

Pole figure

Wide-angle X-ray diffractometer scans were conducted and it is confirmed that the majority of the crystals were α form, though weak reflections for β form or γ form were observed in some cases. We use (040), (110), (130) reflections of α form to investigate crystal orientation of IPP Samples prepared by vibration-injection molding. The reference axes of machine direction (MD), transverse direction (TD) and normal direction (ND) chosen for the samples to be tested are shown in Figure 6.

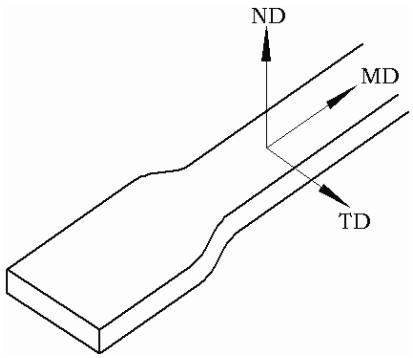

Figure 6. Sketch of part of a sample showing the machine direction (MD), the transverse direction (TD) and the normal direction (ND).

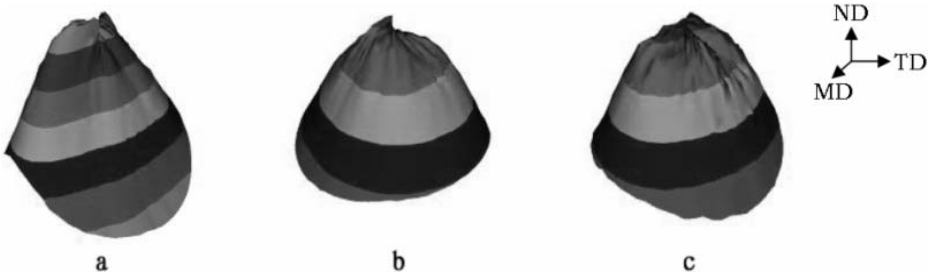

Figure 7. Pole figures of α-PP of static sample. (a) (040)plane, (b) (110)plane, (c) (130)plane

Figure 7 is pole figures of (040)α, (110)α, (130)α reflection of the static sample. The normal of (040)α represents the b axis of α monoclinic, the (040)α pole figure actually exhibits the orientation for b axis. In Figure 7(a), the inner contour has the strongest pole intensity, and the contours are ellipses with small ratios of major axis to minor axis. The contours of Figure 7(b) and (c) are almost circular at large angles. It indicates that the b-axis of the static sample just orientates slightly along M direction (MD).

Figure 8 is pole figures of (040)α, (110)α, (130)α reflection of the sample obtained at T = 230°C, f = 0.5Hz and Pv = 75MPa. The (040) poles have a stronger equatorial orientation than that shown in Figure 7(a), and it is evident that the b-axis is arranged in a cylindrical manner about the MD. At the same time, b-axis has a slight preference orientation about N direction (ND), as there are not any closed contours in the center in the pole-figure. As shown in Figure 8(b), the pole intensity of (110)α plane has the biggest value in the center of the equator, the ND orientation of (110) normal is obvious. In Figure 8(c), the direction of the pole intensity is along MD. Since (130)α plane is parallel to the c axis of α monoclinic, the normal of (130) is perpendicular to the c axis. It is regarded that the c axis has a preferential orientation in T direction (TD).

The sample used in Figure 9 was obtained at T = 190°C, f = 1.5Hz and Pv = 35MPa. From Figure 9(a), the density of the closed contours becomes very high in the center, and few contours cross the excircle. At this condition, the (040) poles show maximum intensities in the ND. As there is no contours cross the excircle in the direction perpendicular to MD, it is not pronounced that the b-axis is primarily oriented along the equatorial bands. It indicates that the b-axis rotates around the ND in a cylindrical manner with a rotating angle between the b-axis and the basic circle below 90°. Compared (110)α, (130)α in Figure 9 with (110)α, (130)α in Figure 8, it can be found

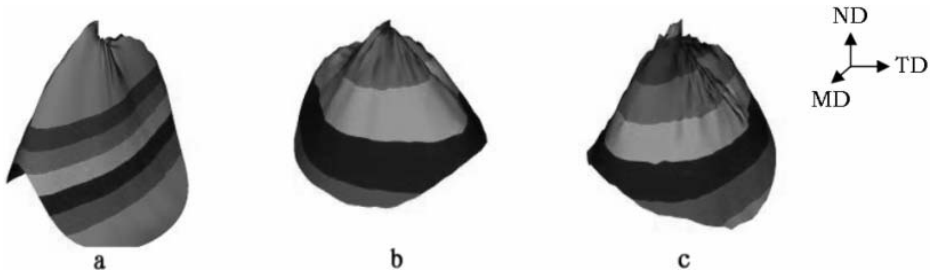

Figure 8. Pole figures of α-PP of sample obtained at T = 230°C, f = 0.5Hz, and Pv = 75MPa. (a) (040)plane, (b) (110)plane, (c) (130)plane

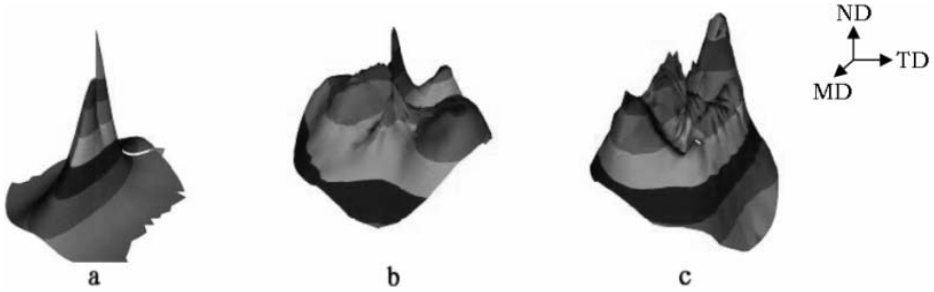

Figure 9. Pole figures of α-PP of sample obtained at T = 190°C, f = 1.5Hz, and Pv = 35MPa. (a) (040)plane, (b) (110)plane, (c) (130)plane

that the pole intensity points are more disperse. Therefore, when melt temperature is 190°C, increasing vibration frequency induce (040)α to arrange parallel to the surface of the sample bar. However, (110)α and (130)α which parallel to c axis do not show preferential orientation in MD or TD respectively.

Polarized microscopic observation

Figure 10 is PM micrograghs of a static sample, and Figure 11 and Figure 12 are PM micrograghs of sample obtained at T = 230°C, f = 0.5Hz, Pv = 75MPa and sample obtained at T = 190°C, f = 1.5Hz, Pv = 35MPa. The specimens for middle layer observation of polarized microscopic were microtome from layers with a distance of 1.5mm to the surface of samples whose thickness was 5mm, while the specimens for core observation from layers with a distance of 2.5mm to the surface. The melt flow direction in Figure 10 and Figure 11 is upright, and that in Figure 12 is expressed as the arrowheads.

Micrograghs of static samples, which are shown in Figure 10, indicate that the crystal structure of iPP samples molded using traditional methods is typical spherulites about 50~60μm in size, and there is no obvious difference between the spherulites in middle layer and the spherulites in core. However, the crystal structure of vibration samples changes. In Figure 11, the spherulites in core are approximately the same as the spherulites shown in Figure 10(a), but those in the middle layer become smaller, say

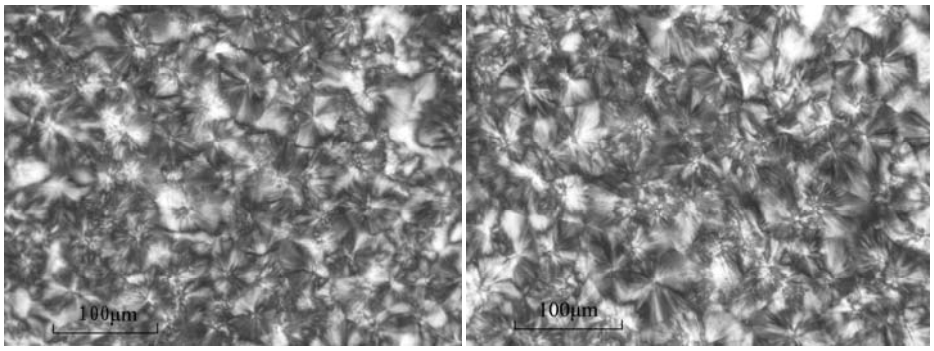

(a) middle layer (b) core

Figure 10. PM microgragh of static sample.

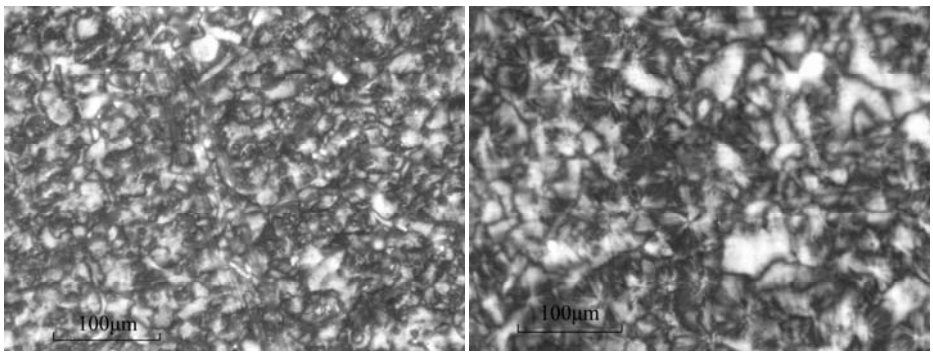

(a) middle layer (b) core

Figure 11. PM micrograph of sample obtained at T = 230°C, f = 0.5Hz and Pv = 75MPa.

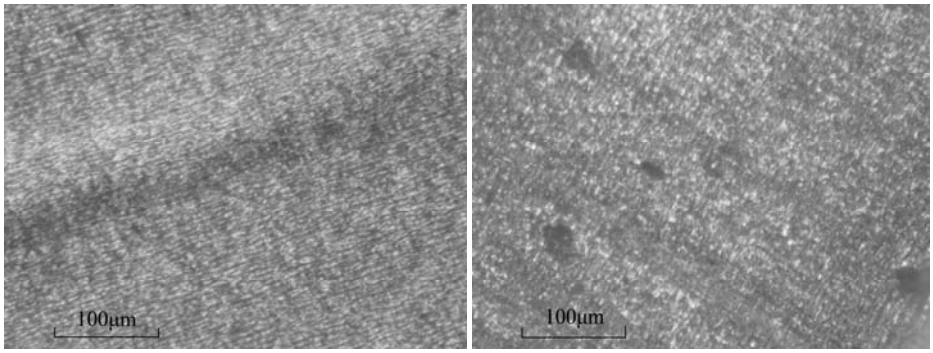

(a) middle layer (b) core

Figure 12. PM micrograph of sample obtained at T = 190°C, f = 1.5Hz, Pv = 35MPa.

about 20~30μm in size. In Figure 12, the crystal is not spherulites, but platelets which become very small and orientate obviously along the direction of melt flow. It indicates that melt vibration makes crystallite orientate and become smaller, especially when vibration frequency is high.

3. Discussion and conclusion

When injected into a mold cavity, polymer melt next to the cavity wall cools quickly to form a solidified polymer layer because of low temperature of the mold, while the core of polymer will stay melting state for a period of time. Consequently the molecular orientation, which is caused by melt flow during the filling time, is ‘‘frozen’’ in the solid layer. On the contrary, the degree of molecular orientation in the core decreases significantly. In addition, because of intense shearing effect in the out layer and weak shearing effect in the core, conventional injection-molding products have a characteristic of high degree of molecular orientation in the out layer and low degree in the core. When vibration is introduced to polymer melt in mold cavity, the

melt is pressed and released periodically to help polymer molecules in inner layer orientate. The orientation is then fixed layer by layer during the cooling time. The degree of molecular orientation in the inner layer of vibration samples has a significant increase compared with that of traditional injection samples. As a result, tensile strength of vibration samples is higher than that of traditional injection samples. Either the increase of vibration frequency or the increase of vibration pressure will intensify vibration effect and make crystal become smaller, so both tensile strength and impact strength of iPP F401 samples increase with the increase of vibration frequency or vibration pressure. From the results we can draw conclusions as follows:

1. Tensile strength of vibration samples increases with the increase of vibration frequency, and the maximum increments are respectively 20.8%, 16.0% and 14.5% at the different melt temperatures of 190°C, 210°C and 230°C.Tensile strength of vibration samples also increases with the increase of vibration pressure, and the maximum tensile strength is obtained under a maximum vibration pressure of 75MPa, the increment is 26.1%.
2. Impact strength of vibration samples increases with the increase of vibration frequency or vibration pressure. It increased significantly under special vibration conditions. For instance, the impact strength of vibration samples, which is molded under the process conditions of T = 190°C, Pv = 75MPa and f = 0.5Hz, has increased by 85% to reach 15.2KJ/m^2 from 8.2KJ/m^2 of no-vibration samples.
3. A high vibration frequency will enable the vicat softening temperature of iPP F401 samples to rise 6~8°C, and vibration pressure has no significant effect on vicat softening temperature.
4. Pole figures show that α-PP of a static sample just orientates slightly along MD, while vibration samples orientate much stronger. The orientation of the normal of (040)α plane of the sample obtained at T = 230°C, f = 0.5Hz and Pv = 75MPa is preferred in MD, and the orientation of the normal of (040)α plane of the sample obtained at T = 190°C, f = 1.5Hz and Pv = 35MPa is preferred in ND.
5. PM micrograghs show that the crystal structures of both static samples and vibration samples obtained at T = 230°C, f = 0.5Hz and Pv = 75MPa are typical spherulites, and the spherulites in static samples are larger in size than that of vibration samples. The crystal structure of vibration samples obtained at T = 190°C, f = 1.5Hz and Pv = 35MPa is “fiber-like” crystalline morphology which orientates along melt flow direction.

Acknowledgments. We would like to express our great thanks to National Basic Research Program of China 2005CB623800, National Natural Science Foundation of China 50473053 and 50533050, and the Scientific Research Foundation for Returned Overseas Chinese Scholars, State Education Ministry, for financial support, and great thanks to Mr. John Harper and Dr. David Ross, IPTME, Loughborough University, UK, for doing pole figure experiments.

References

1. Kalay, Gurhan; Bevis, Michael J. Journal of Polymer Science, Part B: Polymer Physics, 1997, 35(2): 241~263
2. Qing Guan; Kaizhi Shen. Chemical Journal of Chinese Universities, 1995, 16(7): 1133

3. Ibar, J.P. Polymer Engineering and Science, 1998, 38(1): 1~20
4. Jie Zhang; Kaizhi Shen; Yueqin Gao; Yi Yuan. Journal of Applied Polymer Science, 2005, 96(3): 818~823
5. Zheng Yan; Kaizhi Shen; Jie Zhang; Limin Chen; Chixing Zhou. Journal of Applied Polymer Science, 2002, 85(8): 1587~92
6. Jie Zhang; Kaizhi Shen. Journal of Polymer Science, Part B: Polymer Physics, 2004, 42 (12): 2385~2390